Chapter 2
BACKGROUND AND MODELLING APPROACH

1 INTRODUCTION

This chapter describes the generation of a three-dimensional (3-D) model of the implanted cochlea. The objective with the model is to estimate the *electrical potential distributions at the target auditory nerve fibres* caused by current injection into the deaf cochlea. The complex 3-D structure of the cochlea had to be conserved so that the effect of cochlear structures, neighbouring cochlear canals and conduction along the fluid-filled canals of the cochlea could be incorporated in the potential estimates (and thus the neural excitation patterns). The proposed model is classified as a volume conduction model. Since the geometry of the cochlea is complex, accurate analytical solutions for the volume conduction problem, i.e. calculation of potential distributions in the implanted cochlea with closed-form equations, do not exist. Analytical models only give a qualitative insight into the fields generated by intracochlear stimulation (Jolly, Spelman, & Clopton, 1996). Numerical methods are required for an accurate description of field distributions (Steele, 1987). The volume conduction problem of the implanted cochlea is addressed by various numerical methods: lumped parameter (LP) models (Johnstone, Johnstone, & Pugsley, 1966; Kral et al., 1998; Rodenhiser & Spelman, 1995; Strelioff, 1973; Suesserman & Spelman, 1993), finite difference methods (Girzon, 1987), boundary element methods (Briaire & Frijns, 2000; Frijns, de Snoo, & Schoonhoven, 1995) and the finite element (FE) method (Finley, Wilson, & White, 1990; Rattay, Leao, & Felix, 2000).

The FE method was selected for this study because of the ease with which different array locations and electrode configurations could be defined without remeshing the volumes. The model described here is a detailed 3-D spiralling representation of the

first one-and-a-half turns of the implanted cochlea. Electrodes and electrode arrays were simply activated or deactivated by changing the material properties of the applicable elements. The FE model is coupled with a nerve fibre model to translate the potential distributions calculated with the FE model into neural excitation patterns. In this chapter the theoretical background pertaining to the volume conduction problem is discussed, the definition and construction of the model are outlined, and verification methods are presented.

2 THE FINITE ELEMENT MODEL

To determine the potential distributions as a result of intracochlear stimulation, a numerical linear field problem must be solved (Steele, 1987) using the FE method (the method selected for this study). The modelling approach can be broken down into four primary categories: definition of the problem, construction and solution of the FE model, data processing and verification of model integrity and results.

2.1 Definition of the problem

2.1.1 Problem domain and fields to be calculated

The problem domain consists of the cochlea embedded into the surrounding tissues, in this case the temporal bone. The cochlea consists of different tissues each having specific material properties. The problem domain can thus be divided into several subdomains each representing a specific tissue. Each subdomain is characterised by a linear, isotropic conductivity (except the peripheral axonal processes that have anisotropic conductivity). The electrical potential distributions as a result of an injected current have to be calculated at the target nerve fibres.

2.1.2 Equations to be solved

The problem is quasi-static since capacitive, propagation and inductive effects can be neglected (Plonsey, 1969; Steele, 1987) based on the approximation of all

cochlear tissues with purely resistive materials. Simulations are thus performed with low-frequency ac current (0 Hz). As a result, the current density ***J***, the electric field ***E*** and the scalar potential are purely spatial variables, which are directly proportional to the excitation current at any moment in time.

If a current source (stimulation current) I_s is applied, its value equals the divergence of the current density vector ***J***

$$I_s = \nabla \cdot \boldsymbol{J} . \tag{2.1}$$

The electric field is obtained by the negative gradient of the scalar potential , i.e.

$$\boldsymbol{E} = -\nabla\Phi . \tag{2.2}$$

According to Ohm's law the current density ***J*** and the electric field ***E*** are related by

$$\boldsymbol{J} = \frac{1}{\rho}\boldsymbol{E} , \tag{2.3}$$

where is resistivity in -m. Combining (2.1) to (2.3)

$$I_s = \nabla\cdot\boldsymbol{J} = \nabla \cdot (-\frac{1}{\rho}\nabla\Phi) = -\frac{1}{\rho}\nabla^2\Phi \tag{2.4}$$

$$\nabla^2\Phi = -\rho I_s \tag{2.5}$$

which is Poisson's equation for a static potential distribution due to a source I_s.

2.1.3 Boundary conditions

The first boundary condition is applied inside the FE model on the boundaries between cochlear structures. This boundary condition states that potentials $_j$ must

be continuous over boundaries, i.e.

$$\Phi_j = \Phi_{j+1} \tag{2.6}$$

The second boundary condition is applied on the outer boundaries of the model, i.e. on the outside of the bone cylinder. Since the model's outer boundaries (represented by surface **S** in Figure 2.1) are not insulating, current can emerge through them. This implies that the current density must be continuous in the direction normal to the surface **S** (Gonzalez & Huerta, 1979), i.e.

$$\boldsymbol{Jn}_j = \sigma_j \boldsymbol{En}_j = \sigma_j \frac{\partial \Phi_j}{\partial S} = \sigma_{j+1} \frac{\partial \Phi_{j+1}}{\partial S} = \sigma_{j+1} \boldsymbol{En}_{j+1} = \boldsymbol{Jn}_{j+1} \tag{2.7}$$

where $_j$ is the electrical conductivity and *S* is the boundary between different materials j and j+1.

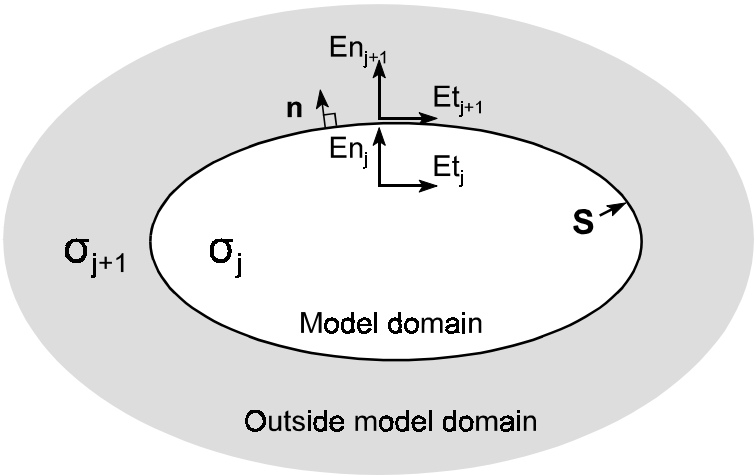

Figure 2.1. Schematic representation of boundary condition on a conducting boundary, i.e. a boundary between two materials where $_j$ and $_{j+1}$ have the same order of magnitude. **n** is a unit vector normal to surface **S**.

The third boundary condition exists on metallic surfaces, i.e. the electrode contacts, in contact with other conducting media, i.e. the cochlear tissues. These surfaces are

defined as equipotential surfaces (Girzon, 1987; Rubinstein, Soma, & Spelman, 1985).

2.2 Construction and solution of the FE model

2.2.1 Software package used

A multi-physics FE software package, *ANSYS*, was used to create the cochlear model. ANSYS uses Poisson's equation (2.5) as the basis for electric field analysis (ANSYS, 1999). Electric scalar potentials are the primary unknowns or nodal degrees of freedom (DOF) that are calculated. A steady-state current conduction analysis was performed to calculate the values of the scalar potential at predefined points on the target nerve fibres as a result of an injected stimulation current.

2.2.2 Elements used

A two-dimensional (2-D) geometry was used to extrude the cochlear structures from (Figure 2.4). This 2-D geometry was generated with 2-D plane elements with four nodes. Since the specific type of element can be used for coupled electrical and thermal analyses, it incorporates both voltage and temperature degrees of freedom at each node. The temperature degree of freedom was not used[1]. Triangular elements could be formed by combining two of the nodes.

The 3-D element used is similar to the 2-D plane element since it also incorporates both temperature and voltage degrees of freedom at its nodes. The temperature degree of freedom was again not active. The 3-D solid element is a brick element defined by 8 nodes and orthotropic material properties. Obtaining prism and tetrahedral element shapes is possible by combining the applicable nodes.

2.2.3 Discretization of model domain

Construction of the cochlear model was performed as follows. A 2-D line drawing of

[1]If the material properties corresponding to a specific degree of freedom are not specified, that degree of freedom becomes inactive.

the geometry of a slice through the cochlea was created through the GUI interface of the FE software package. The geometry is a combination of the geometry used by Finley, Wilson, & White (1990) (Figure 2.2) and a photomicrograph of the cochlea that indicates the position of the spiral ganglion shown in Figure 2.3 (Golden, 1997).

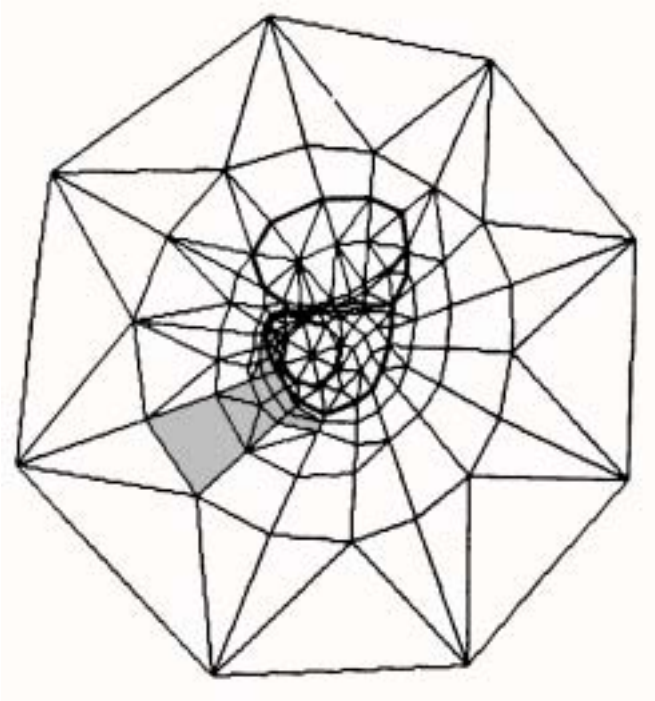

Figure 2.2. 2-D FE geometry used by Finley, Wilson and White (1990).

Different areas, each representing a specific cochlear structure (and thus a tissue), were defined by the lines. The areas were meshed using the plane elements described in section 2.2.2 (Figure 2.4). The 2-D geometry was then extruded into 3-D around the axis of the modiolus (Figure 2.5). To simplify the extrusion process, the diameters of the structures were not tapered toward the apical end of the model. The 3-D solid elements described in section 2.2.2 were used for the extrusion. A cylindrical coordinate system was used for the extrusion and the extrusion parameters are listed in Table 2.1. The first half-turn of the model was generated with 40, the second with 30 and the third with 20 equal *angle* segments.

This produced model segments with approximately equal lengths. Any of the segments could thus be used to construct electrode contacts, allowing the model to be used for different electrode configurations, e.g., pseudo monopolar electrode configurations where the return electrode is located on the opposite side (i.e., in the next half-turn) of the cochlea.

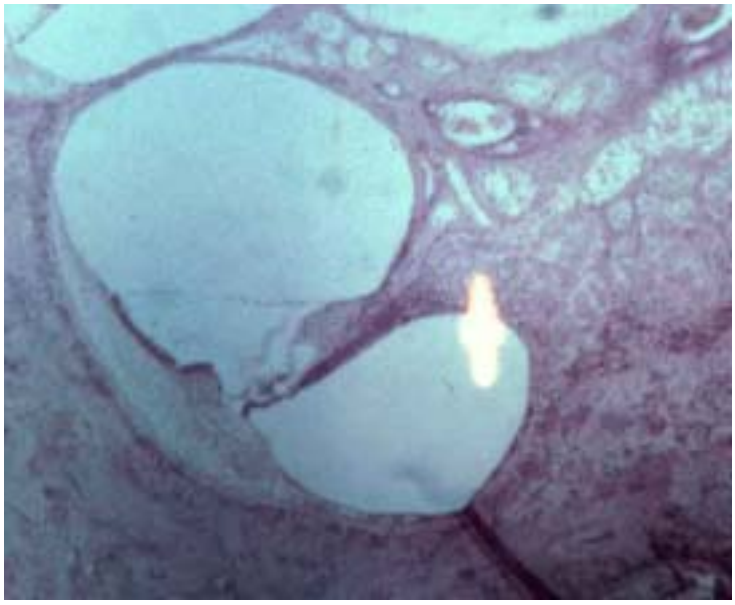

Figure 2.3. Photomicrograph of a section through one turn of the mammalian cochlea (Golden, 1997) that was used in the creation of the 2-D geometry of the FE model.

The method by which the 2-D model in Figure 2.4 was extruded into three dimensions (Figure 2.5) dictated the shape of the modelled spiral ganglion. A layer of axons was created during the extrusion process in the modiolus. The axons were extended so that the nerve fibres originating from the upper half-turn of the model extended downwards to at least below the scala tympani of the lower half-turn of the model. This provided a means of determining which of the axons inside the modiolus might be stimulated as a result of stimulation in the lower turn of the model. To be a true representation of the anatomy the axons should eventually combine into one nerve bundle. In the model this was realized by "filling" the volume enclosed by the medial axonal processes with nerve tissue, i.e. setting the material properties of elements in this volume to that of nerve tissue. The volume of nervous tissue

extends to the end of the bone cylinder thereby creating a low conductance path along the modiolus. Nerve tissue's conductance is approximately twice that of bone. Figure 2.5 does not show the nerve tissue enclosed by the medial axonal processes (which are protruding below the scalae).

2.2.4 Dimensions and anatomical detail of cochlear model

The model approximates the scalae of a human cochlea. However, the location of the modelled spiral ganglion corresponds with the location of the spiral ganglion in a guinea pig cochlea (Figure 2.4). In a human cochlea the spiral ganglion is located more towards the eight o'clock position (Figure 2.2). This inaccuracy should mainly influence absolute threshold current values and not the shape of potential distributions and therefore neural excitation patterns that are calculated with the model.

The modelled width of the scala tympani is 1.46 mm, which is less than 1% smaller than the average width of the human scala tympani measured by Hatsushika et al. (1990). The height of the modelled scala tympani is 1.14 mm, which is within 5% of the average measured height of the human scala tympani[2]. If the model were extruded to two-and-three-quarter turns the total height of the modelled cochlea would have been 6.6 mm and not 5 mm as with a human cochlea (Leeson & Leeson, 1981). The model is therefore approximately 25% higher from base to apex (measured along the modiolus) than a normal human cochlea. The base diameter of the modelled cochlea is approximately 8.5 mm which is within 6% of the 9 mm diameter reported by Leeson and Leeson (1981).

[2]The measured width of a number of scalae tympani in human cochleas varied from 3 mm at the base to 1.24 mm at a point 25 mm from the round window and the height between 2.4 mm and 0.8 mm over the same length of the scala tympani (Hatsushika et al., 1990).

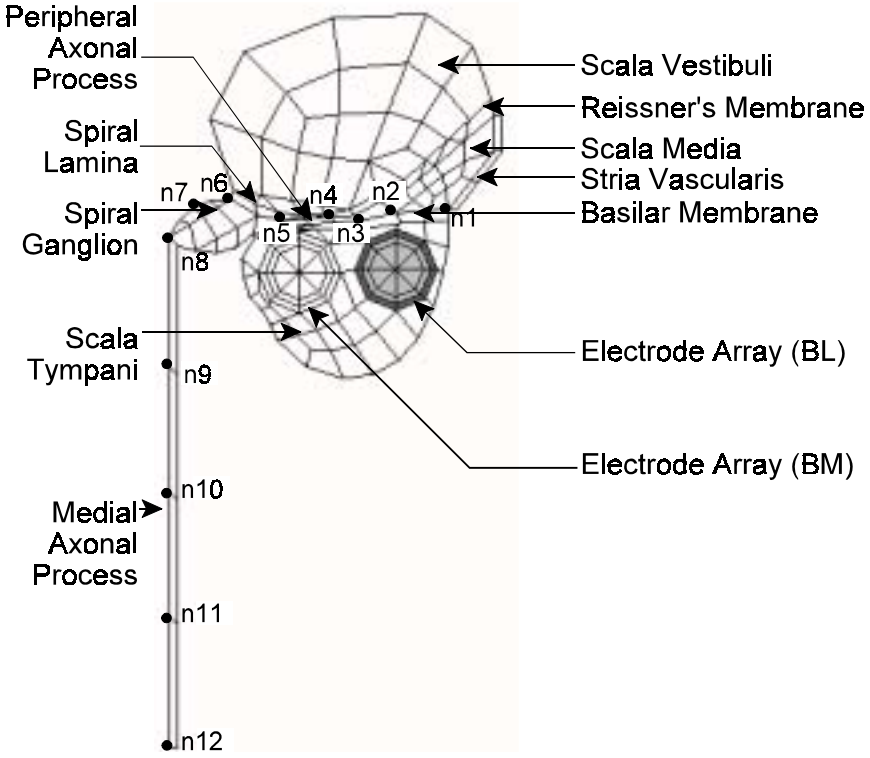

Figure 2.4. 2-D FE model geometry of a plane through one arch of the cochlea. The medial array (marked BM) can be seen as a circular geometry toward the top left of the scala tympani while the lateral array (marked BL) is located toward the top right of the scala tympani and is shaded in this illustration for clarity.

The length of the basilar membrane is 9.2 mm in the first half-turn of the cochlear model, 7.4 mm in the second half-turn and 5.6 mm in the third half-turn (i.e. a total length of 22.2 mm for the first one-and-a-half turns). If the extrusion were to be continued to two-and-three-quarter turns, the total length of the modelled basilar membrane would have been 28.6 mm. Although this is shorter than the average length of the cochlear duct (35 mm reported by Skinner et al. (1994)), Ulehlova, Voldrich and Janisch (1987) reported human cochlear duct lengths of between 28 and 40 mm. It is thus concluded that the dimensions used for the width and height of the cochlear model are representative of a typical human scala tympani.

Table 2.1. Extrusion parameters for 3-D model. Cylindrical coordinates r, and z are used.

[a] The segments per volume refer to the number of sections along the length of the modelled basilar membrane in a single volume extrusion, i.e. in the first half-turn two layers of elements are generated in each 9° volume slice while only one layer of elements is generated in the third half-turn in each volume slice.

Cochlear half-turn	Segments per volume[a]	Total number of volume segments	Total number of segments	r (mm)	(deg)	z (mm)
1st	2	20	40	-0.03	9	0.06
2nd	2	15	30	-0.04	12	0.08
3rd	1	20	20	-0.03	9	0.06

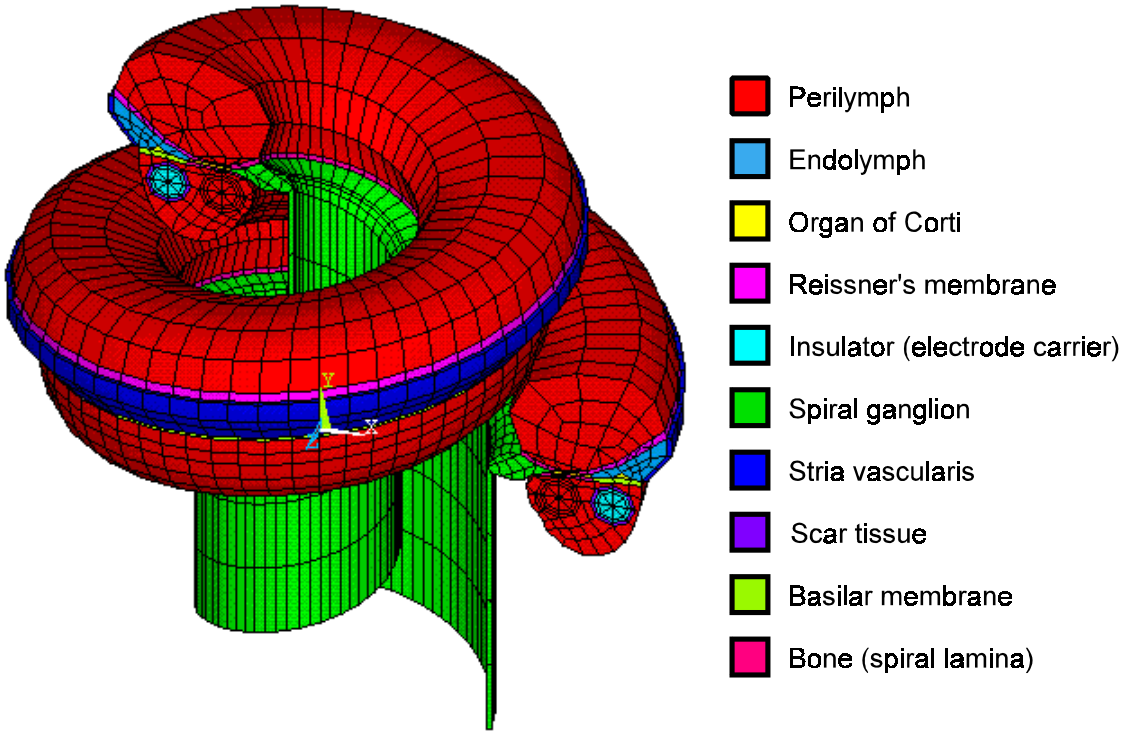

Figure 2.5. 3-D FE model geometry with nerve tissue (that was used to fill the modiolus) and surrounding bone tissue removed. Each colour represents a tissue or material type as indicated in the figure.

Shepherd et al. (1985) recorded insertion depths with a Nucleus electrode in human cadaver cochleas of between 15.5 and 27 mm with a mean insertion depth of 18.6 mm. Since the length of the modelled part of the cochlea is 22.17 mm, it will in most cases represent a cochlea with full electrode insertion. Anatomical studies showed that the straight Nucleus[3] electrode array is positioned approximately 1.0 mm from the modiolus at the extreme base of the scala and 0.8 mm 25 mm from the base (Shepherd, Hatsushika, & Clark, 1993) because of the tapering of the cochlea toward the apex. Other electrodes, e.g. the electrode used in the Clarion implant (Kessler, 1999), are designed to fit snugly around the modiolus. Although such a design does not guarantee a perimodiolar array location, an additional electrode positioner that can force the electrode array to the correct location has recently been developed (Advanced Bionics Corporation, 2000). For this reason the model was designed to allow two possible electrode array locations in the FE model, one close to the modiolus and one at a more lateral location distal to the nerve fibres. The abbreviations for the banded electrode arrays are shown in Figure 2.4 to indicate the two locations: BM indicates the *b*anded *m*edial electrode array and BL indicates the *b*anded *l*ateral electrode array. The distance from the modiolus remained constant over the entire length of the scala tympani for both electrode arrays.

Each electrode in the model consists of a cylindrical core and two external layers (Figure 2.4). Segments of the layer in direct contact with the core were defined as band electrode contacts by setting the resistivity of these segments to that of a conductor. The material properties of the outer layer were set to those of perilymph or scar tissue for this case. The outer layer was also used to create point electrode contacts. Material properties of the remaining part of the outer layer, the inner layer and the core were set to that of an insulator when modelling point electrodes.

[3]The Nucleus implant (Clark, 1996) is a cochlear implant manufactured by Cochlear Corporation.

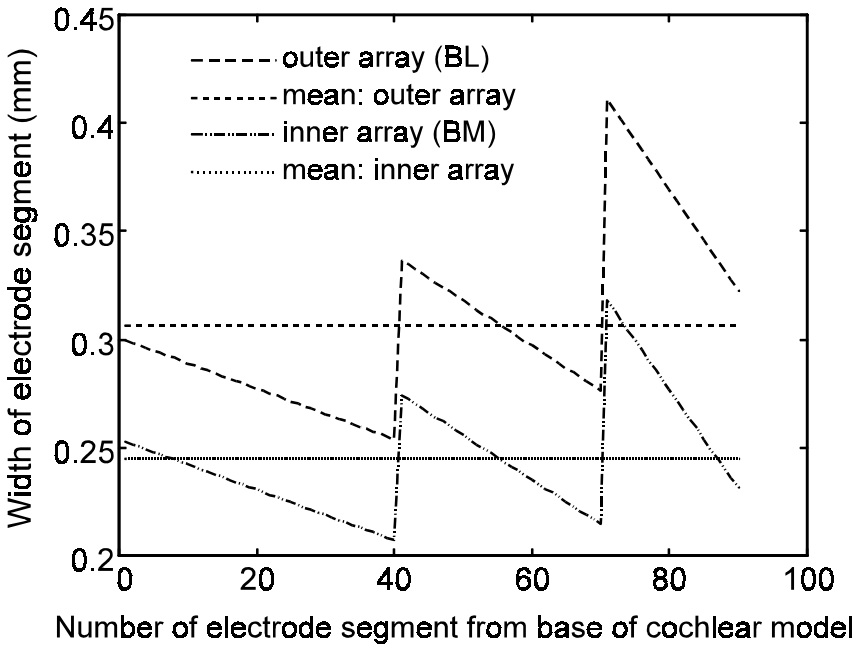

Figure 2.6. Electrode length as a function of position (and thus segment number) along the length of the scala tympani of the modelled cochlea.

The lengths of the electrode contacts varied because of the constant angles of extrusion over each half turn (Figure 2.6). For the inner array the length varied between 0.21 mm and 0.32 mm (approximately 35% relative to the widest section) and for the outer array between 0.25 mm and 0.41 mm (approximately 39% relative to the widest section). However, the variation within one half-turn over the first two half-turns did not exceed 17% for the medial electrode and 15% for the lateral electrode relative to the widest section in each half-turn. The expected effect of this variation is slightly unbalanced current densities on the two electrodes in an electrode pair, resulting in slightly elevated threshold currents for the electrode possessing the larger surface area. No compensation for this effect was made during the calculation of results.

The model was completed by "embedding" the cochlear spiral into a cylinder of bone with a radius of 5.5 mm and depth of 10 mm. Figure 2.7 shows the outlines of the

cochlear spiral embedded into the bone cylinder. The bone cylinder was automatically meshed by the software package. In total, 64 019 elements were generated.

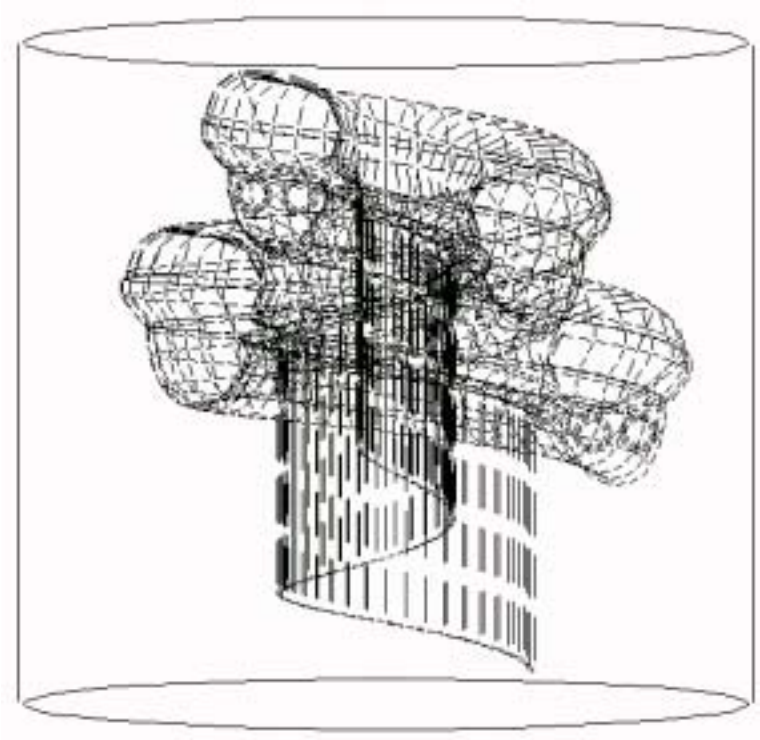

Figure 2.7. Location of cochlear model in bone cylinder.

2.2.5 Material properties

The materials in the model are, as a first approximation, purely resistive because it has been shown that the cochlear tissue impedances are well approximated by pure resistances (Black, Clark, & Patrick, 1981; Spelman et al., 1980; Spelman, Clopton, & Pfingst, 1982). Material properties (Table 2.2) are the same as those used by Finley, Wilson and White (1990), Frijns et al. (Frijns, de Snoo, & Schoonhoven, 1995), Strelioff (1973) and Grill and Mortimer (1994). Estimations of the *in vivo* thicknesses of the basilar membrane, Reissner's membrane and the stria vascularis are based on a mammalian (guinea-pig) cochlea and are 4 m, 1.7 m and 40 m respectively. To obtain well-shaped elements, the thicknesses of these membranes have been scaled up to 80 m, 50 m and 60 m respectively and therefore the

membrane resistivities were scaled down with factors 20, 30 and 1.5.

Table 2.2. Material properties of components in the cochlear model. The resistivity-values for the basilar membrane, Reissner's membrane and the stria vascularis are scaled down by factors 20, 30 and 1.5 respectively from the real values to correct for the increased thicknesses of the membranes in the model. All values are given in -mm.

Model Component	Resistivity (-mm)
Silicone rubber	1 010
Electrode metal	1
Perilymph (scalae tympani and vestibuli)	700
Endolymph (scala media)	600
Bone	6 410
Spiral ganglion	3 000
Peripheral axonal process (anisotropic)	3 000 axial 15 000 transverse
Reissner's membrane	340 130
Basilar membrane	4 000
Stria vascularis	125 790
Organ of Corti	83 333
Fibrous scar tissue	6 270

2.2.6 Source definition and boundary conditions

Electrical stimulation is performed with current stimuli. Since the material properties are purely resistive and the potential distributions could thus be scaled proportional to the source to create biphasic stimuli, a dc current was used as source. To create a uniform current density on the electrode contacts, the nodes of the elements constituting the contacts had to be coupled in the volt DOF. This defined the surface of the electrode contact as an equipotential surface. The full current was then applied onto the primary node in the coupled set. Boundary conditions were in the

form of DOF constraints, i.e. specific voltage values (e.g. 0 V) or voltage constraints (e.g. the continuity constraint between ohmic conductors in equation 2.6) on selected nodes.

2.2.7 Solution

To obtain a solution, the static solution option of the software package was selected. The default frontal solver of the FE software package was used. The solution of one simulation took approximately one hour on a Pentium II 300 MHz personal computer with 500 MB RAM.

2.3 Postprocessing

The FE software's postprocessing module was used to access the calculated scalar electric potential. Potential values at the nodes shown in Figure 2.4 on each segment of the FE model were written to a file. The data went through a number of processing steps before it was ready to serve as input to a nerve fibre model (section 3 in this chapter). Programs written in C were mostly used to process data while Matlab scripts were mostly used to plot results. A schematic representation of the data flow is shown in Figure 2.8.

First, a custom C-program was used to sort the nodal data into 12 sets of data corresponding to the 12 nodes shown in Figure 2.4. Each set of nodal data contained 91 values corresponding to the nodal locations on the intersections of the 90 segments of the model and the two outside planes at the most basal and most apical sections. Next the data were processed by a Matlab script to plot the potential distributions and activating functions (Rattay, 1999) as a function of distance along the basilar membrane and distance along the length of the nerve fibres. The data were also linearly interpolated to obtain potential values at the node locations in the model of a specific nerve fibre (section 3 in this chapter). The final output from this Matlab program was a text file containing the potential values along the length of each nerve fibre. This text file served as input to the C program containing the nerve fibre model.

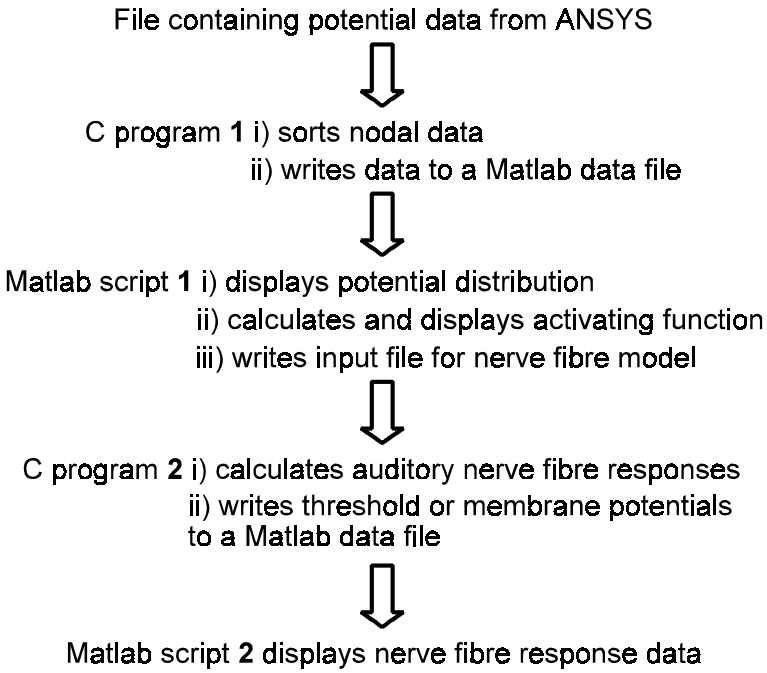

Figure 2.8. Schematic representation of data flow in the simulation of the implanted cochlea

2.4 Integrity and verification of the FE model

The integrity of the FE model was determined by (1) an assessment of the accuracy of the FE method for calculation of the electric potential and the effect of poorly shaped elements on model results, (2) a qualitative assessment of potential distributions as a result of a specific source current distribution that can be compared to results obtained with the FE model. The first aspect was addressed with an FE test problem, while the latter was addressed with analytical and LP models.

2.4.1 FE test problem

The generated mesh is one of the most important parts of the analysis since it affects the accuracy and economy of the analysis (ANSYS, 1997). The error made is a function of the equation solved over the element, the shape of the element, i.e. aspect ratio and angle between adjacent edges, and the type of element, e.g. linear or higher order. 3-D linear conduction elements were used to create the model.

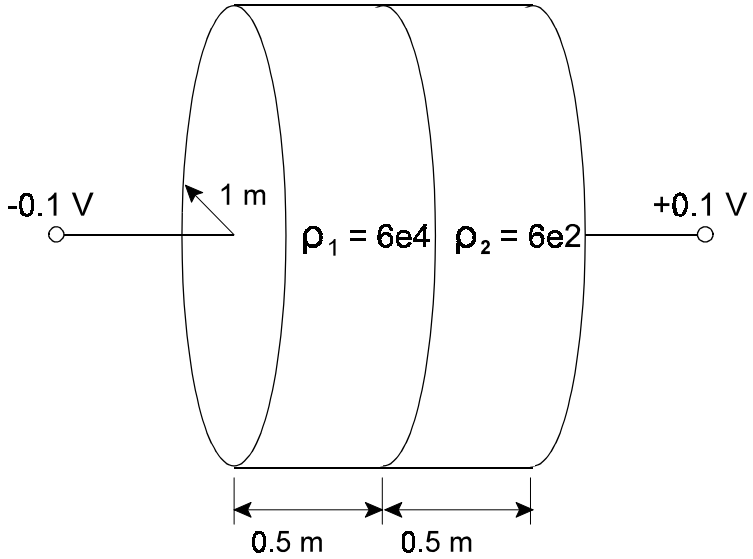

Figure 2.9. Geometry of test problem to verify the results obtained with the FE analysis.

Since the cochlear model has a complicated geometry, only a qualitative verification of the results obtained with the FE model could be done by comparison with analytically calculated values. A first step toward the verification of results obtained from a model with a complex geometry is the modelling of a simple sample problem of which the analysis results are compared with a hand-calculated solution of the same problem.

The test problem consists of two material disks having 1 m radii and 0.5 m thicknesses that were connected as shown in Figure 2.9. On the one end of the composite disk a potential of -0.1 V was applied and on the other side a potential of +0.1 V. The circular surfaces onto which the potentials were applied were assumed to be equipotential surfaces, i.e. perfectly conducting. The resistivities of the two materials were $6x10^4$ -m and $6x10^2$ -m respectively. The materials were assumed to be linear and isotropic and fringing effects were neglected. The hand calculated value for the voltage at the interface of the two materials is 0.09802 V and the worst value calculated by the FE software is 0.09801 V, which differs by 0.01% from the

calculated value. All the elements were well shaped. Since this is more accurate than the dimensional accuracy of the model, the accuracy of the analysis results with well-shaped elements was judged to be adequate.

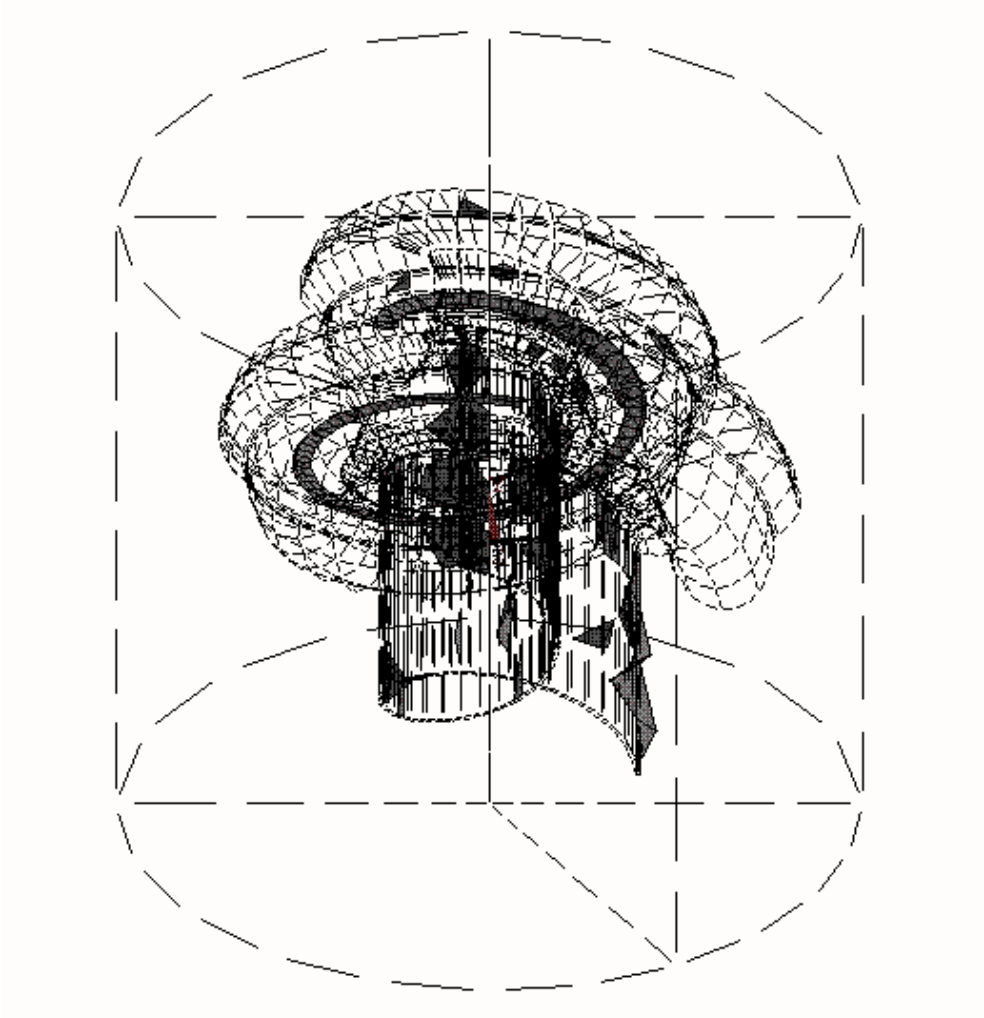

Figure 2.10. Location of poorly shaped elements in the FE model. Poorly shaped elements are shaded while well shaped elements are not shown.

To compensate for the potential loss in accuracy by using linear elements and some poorly shaped elements, a fine mesh with many elements was used to build the cochlear model. Out of the 64 019 elements, 245 tetrahedron elements in the bone cylinder were poorly shaped with the maximum aspect ratio warning issued at 42.73, which exceeds the software's default warning limit of 20, and the maximum angle

between adjacent edges was 172.5 degrees, which exceeds the warning limit of 165 degrees (Figure 2.10). In the cochlear part of the model there are a further 108 poorly shaped elements of which the maximum aspect ratio is 25.66 and the maximum angle between adjacent edges is 172.8 degrees. However, the limits of 20 for aspect ratio and 165 degrees for the angle between adjacent edges are only default guidelines provided by the software program and are also suitable for restrictive types of analyses, e.g. mechanical stress analyses.

Magnetic or electrical analyses typically do not suffer severe effects from poorly shaped elements (ANSYS, 1997). The analyses performed in this study were electrical conduction analyses which are less sensitive to element shape than, for example, structural analyses. The effect of poorly shaped elements located in a critical region is also more likely to be detrimental. Elements that produced shape warnings were mostly located along the centre of the modiolus part of the model, in the bone segment (spiral lamina) between the spiral ganglion and peripheral axonal process and the scala tympani and in the scala tympani between the inner electrode and the bone segment described above. The poorly shaped elements in the bone segment have aspect ratios not exceeding 25.66 and the poorly shaped elements in the scala tympani have aspect ratios not exceeding 22.55. Both these extreme aspect ratios are approaching the limit of 20.

To test the effect of poorly shaped elements, the test problem described above was used again and the elements were narrowed by a factor 100 so that all the elements were poorly shaped. The best shaped elements had an aspect ratio of 30.75 and the worst shaped elements an aspect ratio of 60.12. The maximum error in the analysis differed by 0.03% from the hand-calculated values. From this comparison it is obvious that the element distortion that occurs in the cochlear model is not detrimental to the results of the analyses.

2.4.2 Analytical model

An analytical model (Jolly, Spelman, & Clopton, 1996) of the implanted cochlea was

used to evaluate the potential distributions generated with the FE model (Figure 2.11) qualitatively. In the analytical model the electrical potential V at a location (x,y,z) is a simple superposition of the potential fields of different point current sources evaluated at the location (x,y,z) in a homogeneous isotropic conductive medium, i.e.

$$V(x,y,z) = \sum_{k=1}^{n} V_k , \tag{2.8}$$

where V_k is the potential field as a result of point current source k. The equation can be rewritten in terms of each current source as

$$V(x,y,z) = \sum_{k=1}^{n} \frac{I_k \rho}{4\pi} \frac{1}{R_k} , \tag{2.9}$$

where I_k is the value of the kth current source, is the resistivity of the medium and R_k is the distance from the point where the potential is being evaluated to the location of the kth current source.

The analytical model is used to evaluate the shape of potential distributions as a result of specific electrode configurations and array locations. A normalized value of the potential was therefore calculated by setting $\frac{\rho}{4\pi}$ equal to one. The normalized potential was thus given by

$$V_N(x,y,z) = \sum_{k=1}^{n} \frac{I_k}{R_k} \tag{2.10}$$

For the analytical model the location of the lateral array was defined as on the x-axis (y=z=0) while the location of the medial array was defined as parallel to the x-axis at y=0.5 and z=0. Potential distributions were calculated at a distance of 0.5 mm above the electrode array, i.e. on the plane z=0.5. The z=0.5 plane represented the surface containing the nerve fibres in the FE model (Figure 2.4). Values for the potential field were calculated at the same coordinates along the basilar membrane and along the

nerve fibres as for the FE model to facilitate calculation of electrical tuning curves[4] for both solutions.

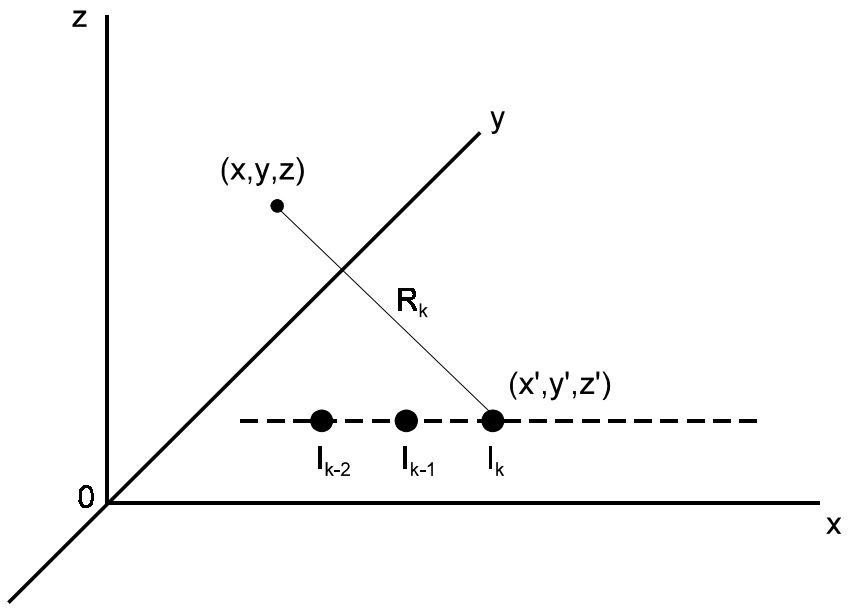

Figure 2.11. Diagram to illustrate the variables in the analytical model of the implanted cochlea. The potential at the field point (x,y,z) is the sum of the potential fields from the current sources I_{k-2}, I_{k-1} and I_k. The source point at I_k is given by (x',y',z'). The distance R_k is given by $R_k = \sqrt{(x-x')^2 + (y-y')^2 + (z-z')^2}$. The dashed line indicates the location of the electrode array; the x-axis is parallel to the basilar membrane; the y-axis is parallel to the nerve fibres and the z-axis represents the radial distance from the nerve fibres.

This formulation of the problem does not take electrode geometries other than point sources, i.e. banded electrode geometries (Chapter 3) and pseudo-continuous

[4] Electrical tuning curves give an indication of the spread of activation by showing the threshold for activation for modelled nerve fibres as a function of distance along the length of the basilar membrane. Electrical tuning curves are calculated by determining the threshold currents of an array of nerve fibres as a result of stimulation with a fixed electrode pair.

electrode geometries (Chapter 5), into account. The model also does not take the 3-D orientation of the electrodes relative to one another as a result of the cochlear geometry into account.

2.4.3 Lumped parameter models

LP models describe the structure of the cochlea with a network of resistive and capacitive components. The most well-known LP model is the transmission line model of the cochlea created by Strelioff (1973). Although LP models mostly do not take the 3-D orientation of the cochlear turns relative to one another into consideration, they are helpful to provide (1) an estimate of the potential distributions of the implanted cochlea for verification purposes and (2) a qualitative insight into some aspects of the volume conduction problem. An LP model is used in Chapter 3 to exemplify the effect of encapsulation tissue around implanted electrodes. The structure and parameters of the model are presented in Chapter 3.

3 THE NERVE FIBRE MODEL

3.1 Interfacing the FE and nerve fibre models

Since the FE model is spiralling, it is not possible to select a plane through it that will intersect all the neural elements in the same position. Consequently, and to compare model results with results and data in literature, a curved surface following the curve of the nerve fibres and spiralling along the length of the basilar membrane was defined (superior and medial surfaces of the structures shown in Figure 2.12). A simplified representation of this surface is shown in Figure 2.13a. Equipotential lines on this curved surface are displayed as contours along the length of the basilar membrane and along the length of the neural elements (Figure 2.13b). The abscissa represents the length of the basilar membrane from the round window (0 mm) to the end of the third half-turn of the cochlea (approximately 22 mm). The nerve fibre terminals are located at 0 mm (near the organ of Corti) and the medial axonal processes end at approximately 3.5 mm (inside the auditory nerve) on the ordinate.

The activating function was used to obtain a first impression of excitation patterns. The activating function is the direct stimulating influence of an extracellular potential on the n^{th} compartment (or node as used in this thesis) of the nerve fibre model (Rattay, 1999). The formulation of the activating function for a bipolar unmyelinated neuron with constant diameter but varying internodal length is given by

$$f_n = \left[\frac{V_{e,n-1} - V_{e,n}}{R_{n-1}} + \frac{V_{e,n+1} - V_{e,n}}{R_n} \right] / C_{m,n} \qquad (2.11)$$

where $V_{e,n}$ is the extracellular potential at the n^{th} node, R_n is the axoplasmic resistance to the next node and $C_{m,n}$ is the nodal membrane capacitance. The activating function was calculated for a fibre with internodal segment lengths corresponding to those of the GSEF model (Table 2.4). Since the first and last nodes do not have neighbouring fibre sections, a reduced form of (2.11) was used to calculate the activating function at these nodes.

The activating function is normally used to indicate the location along the length of a nerve fibre where activation is likely to occur. However, the exact site of activation of a nerve fibre was not relevant in this study. Excitation profiles[5] were calculated by detecting propagating action potentials at the 16th node of the modelled nerve fibres. Activating functions were thus used to determine the regions along the basilar membrane where excitation is most likely to occur, i.e. the selection of nerve fibres that are most likely to exibit propagating action potentials under specific stimulation conditions.

Contour plots of the activating function (hereafter called AF contours) over the curved surface defined above were used to calculate possible regions of excitation. A comparison between the AF contours generated for different electrode configurations

[5] Excitation profiles are the same as electrical tuning curves or spatial tuning curves, as used by some authors. In this thesis the terms "excitation profile" and "electrical tuning curve" is used interchangeably.

using the same stimulus intensities can also provide an indication of the effectiveness of stimulation since the intensity of the activating function gives an indication of the relative threshold that can be expected, i.e. a lower value of the activating function corresponds to a higher threshold current and a higher value of the activating function corresponds to a lower threshold current. Also, it it important to realize that when biphasic stimuli are used, maxima and minima in AF contours both indicate possible regions of excitation.

3.2 Modelling of auditory nerve excitation

The FE model of the cochlea consisted of 90 segments. Electrical potentials were calculated on the boundaries of the segments producing 91 sets of potential values. Consequently 91 nerve fibres were modelled. If a uniform nerve fibre density of 13 600 nerve fibres per cochlear turn[6] is assumed throughout the modelled cochlea, each modelled nerve fibre represents approximately 224 real nerve fibres.

Neural excitation patterns in the spiralling model were determined using the generalized SEF (GSEF) auditory nerve fibre model described by Frijns, de Snoo and Schoonhoven (1995). The GSEF model, an active model of an auditory nerve fibre, describes a myelinated nerve fibre with 15 segments (16 nodes) and is an active cable model of a guinea pig high spontaneous rate fibre. Potential values at the location of the 16 nodes in the GSEF nerve fibre model were calculated by interpolation of the potential values at the 12 nodes in the FE model. The first node in the GSEF model corresponds to node n_3 in the FE model. The potential values calculated with the FE model were thus applied as external excitation potentials on the nodes of 91 modelled nerve fibres.

[6] Calculated from Spoendlin and Schrott (1989) based on a cochlear length of 30 mm.

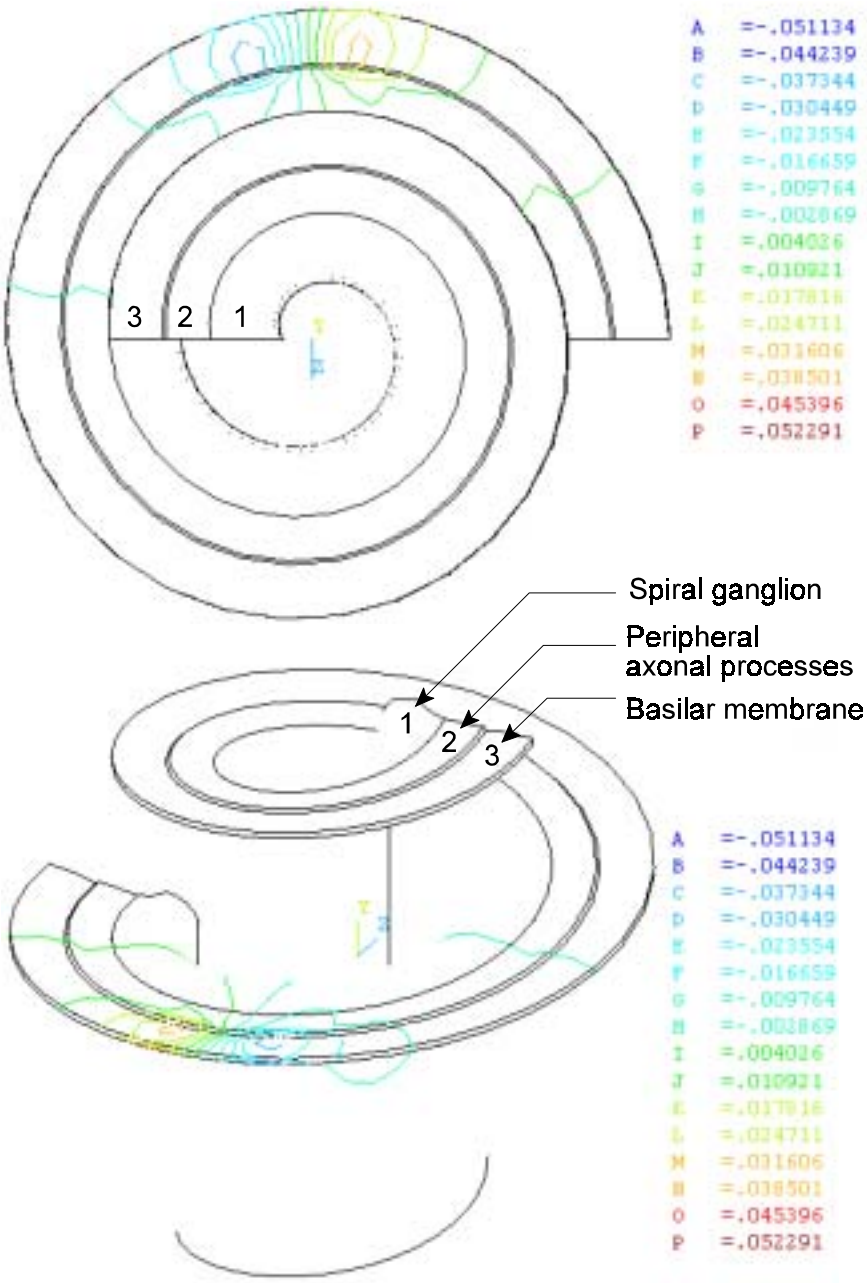

Figure 2.12. Top view (upper figure) and oblique view (lower figure) of spiral ganglion, peripheral axonal processes and basilar membrane of the FE model over which potential distributions were calculated. Equipotential lines are shown for a BP electrode configuration for the BM array.

The GSEF model is based on the original Frankenhaeuser-Huxley (FH) model (Frankenhaeuser & Huxley, 1964) which describes the membrane kinetics of the myelinated nerve fibre of the frog. Schwartz and Eikhof (1987) adjusted the FH model to represent mammalian nerve fibres which resulted in the Schwartz-Eikhof (SE) model for myelinated nerve fibres of the rat. Frijns (1995) adapted this model to represent a high spontaneous rate auditory nerve fibre based on measurements made on the guinea pig.

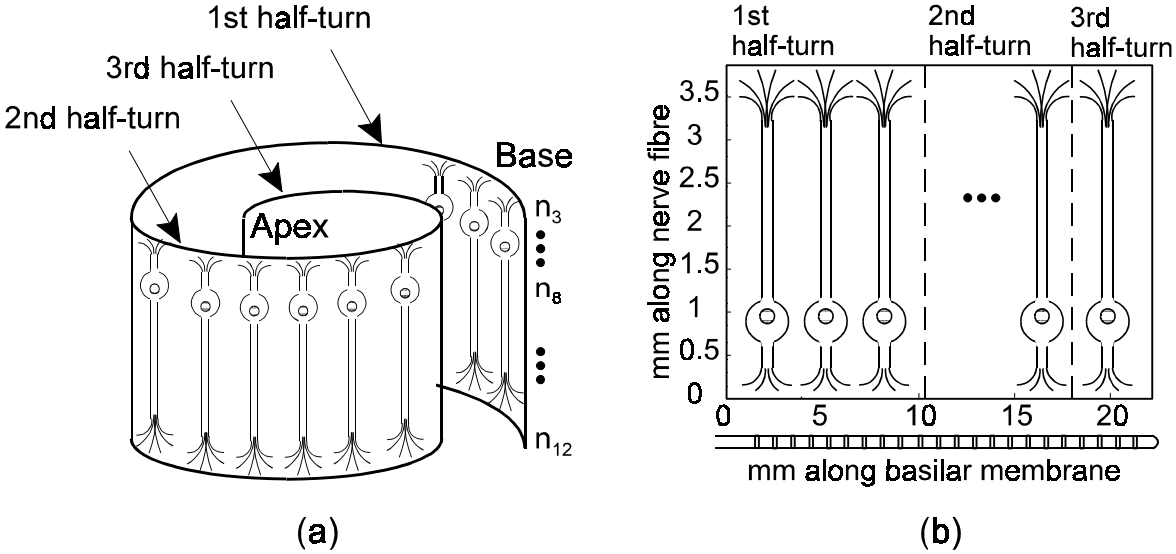

Figure 2.13. (a) A simplified diagram to illustrate the location of the plane in the FE model where the potential distributions are displayed. Nodes n_3 to n_{12} at the right of the figure correspond with the nodes in the FE model Figure 2.4. (b) The orientation of the nerve fibres and the basilar membrane on the potential distribution plots.

Although there are differences between human and guinea-pig nerve fibres, e.g., the myelinated cell body of the guinea-pig nerve fibre versus the unmyelinated cell body of the human nerve fibre, the model is used to make a *relative* assessment of the excitation properties of various electrode locations, configurations and geometries. Threshold currents vary considerably among implant users as a result of a number of inter-person variations such as variations in cochlear geometry, nerve fibre survival

patterns and electrode location, geometry and configuration. Variations in threshold currents that occur as a result of the use of a guinea-pig fibre are, as a first-order approximation, considered to be comparable to inter-person variations. Because of the use of a guinea-pig fibre, the exact site of excitation along the length of the nerve fibre is not considered in this study. To determine threshold currents, the presence or absence of a propagating action potential is used as measure.

Three nodes (k-1, k, k+1) of the GSEF cable model are shown schematically in Figure 2.14. The membrane potential is a function of the membrane's permeability to ions (P_{Na} and P_K in Figure 2.14), membrane capacitance C_m, nonspecific nodal leak current as a result of the leak conductance $G_{L,k}$, axial conduction through the axoplasmic conductance $G_{a,k}$ and externally applied electric fields $V_{e,k}$.

A uniform, finite length, active cable model of a nerve fibre with N nodes is described by the following coupled differential equations (Frijns, de Snoo, & Schoonhoven, 1995):

$$\frac{dV_1}{dt} = \frac{1}{C_m}\ [-(G_{a,1} + G_{L,1})\cdot V_1 + G_{a,k}\cdot V_2 + -(G_{a,1})\cdot V_{e,1} + G_{a,1}\cdot V_{e,2} + I_{act,1} + I_{L,1}] \quad (2.12)$$

for node 1,

$$\frac{dV_k}{dt} = \frac{1}{C_m}\ [G_{a,k-1}\cdot V_{k-1} - (G_{a,k-1} + G_{a,k} + G_{L,k})\cdot V_k + G_{a,k}\cdot V_{k+1} + G_{a,k-1}\cdot V_{e,k-1} - (G_{a,k-1} + G_{a,k})\cdot V_{e,k} + G_{a,k}\cdot V_{e,k+1} + I_{act,k} + I_{L,k}] \quad (2.13)$$

for nodes 2 to N-1, and

$$\frac{dV_N}{dt} = \frac{1}{C_m}\ [G_{a,N-1}\cdot V_{N-1} - (G_{a,N-1} + G_{L,N})\cdot V_N + G_{a,N-1}\cdot V_{e,N-1} - (G_{a,N-1})\cdot V_{e,N} + I_{act,N} + I_{L,N}] \tag{2.14}$$

for node N. V_k is the deviation of the membrane potential from the resting membrane potential, V_r.

The active current per node, I_{act}, is the sum of the active sodium and potassium currents per node

$$I_{act,k} = I_{Na,k} + I_{K,k} \tag{2.15}$$

where

$$I_{Na,k} = P_{Na,k} h_k m_k^3 \cdot \frac{E_k F^2}{RT} \cdot \frac{[Na^+]_o - [Na^+]_i \cdot \exp(\frac{E_k F}{RT})}{1 - \exp(\frac{E_k F}{RT})} \tag{2.16}$$

and P_{Na} is the nodal sodium permeability, h and m are the probabilities for opening the Na^+ ionic channels, $E_k = V_k + V_r$ is the transmembrane potential, $[Na^+]_o$ is the extracellular sodium concentration, $[Na^+]_i$ is the intracellular sodium concentration, T is the absolute temperature, F is Faraday's constant and R is the gas constant.

The equation for $I_{K,k}$ is similar to the equation for $I_{Na,k}$ and is given by

$$I_{K,k} = P_{K,k} n_k^2 \cdot \frac{E_k F^2}{RT} \cdot \frac{[K^+]_o - [K^+]_i \cdot \exp(\frac{E_k F}{RT})}{1 - \exp(\frac{E_k F}{RT})} \tag{2.17}$$

where P_K is the nodal potassium permeability, n is the probability for opening the K^+ ionic channels, $[K^+]_o$ is the extracellular potassium concentration and $[K^+]_i$ is the

intracellular potassium concentration.

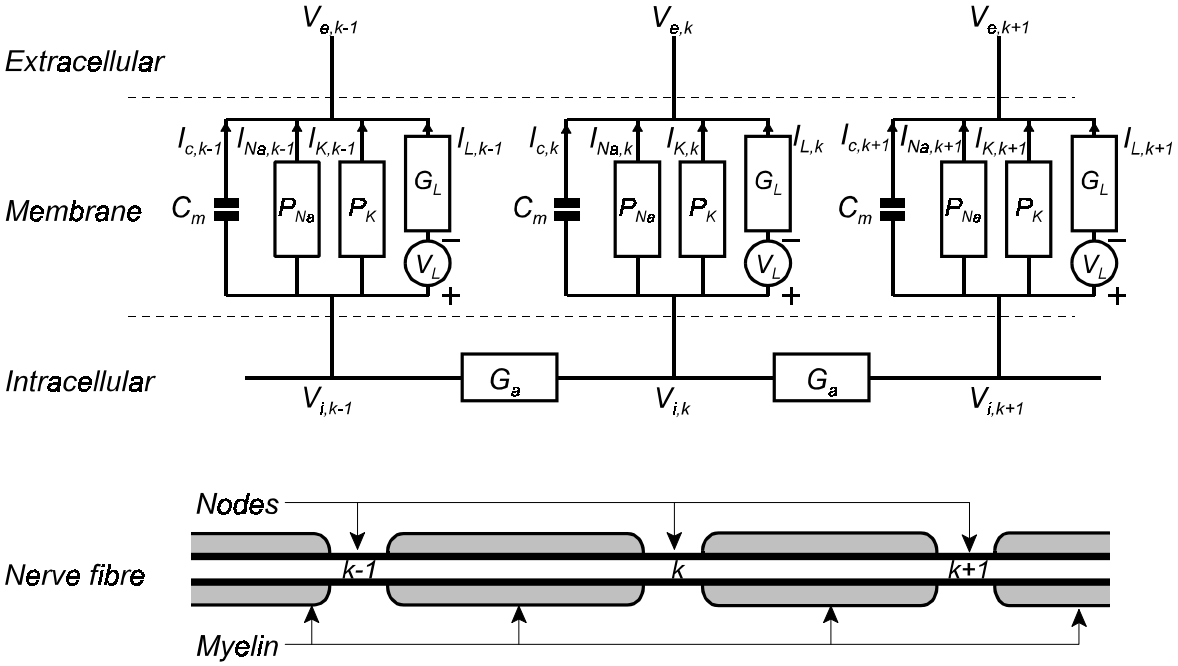

Figure 2.14. Schematic representation of three nodes in the GSEF model of a myelinated auditory nerve fibre. The lower part of the figure shows the physical structure of the section of myelinated nerve fibre of which the circuit representation is shown in the upper part of the figure. The reader is referred to the text for a description of the parameters.

The resting membrane potential V_r is calculated with the Goldman equation

$$V_r = \frac{RT}{F} \cdot \ln\left(\frac{P_K n_0^2 [K^+]_o + P_{Na} h_0 m_0^3 [Na^+]_o}{P_K n_0^2 [K^+]_i + P_{Na} h_0 m_0^3 [Na^+]_i} \right) \tag{2.18}$$

m, n and h are calculated by the following set of differential equations:

$$\frac{dm_k}{dt} = [-(\alpha_{m,k} + \beta_{m,k}) \cdot m_k + \alpha_{m,k}]$$
$$\frac{dn_k}{dt} = [-(\alpha_{n,k} + \beta_{n,k}) \cdot n_k + \alpha_{n,k}] \quad (2.19)$$
$$\frac{dh_k}{dt} = [-(\alpha_{h,k} + \beta_{h,k}) \cdot h_k + \alpha_{h,k}]$$

where

$$\alpha_{m,k} = \frac{A_{\alpha_m}(V_k - B_{\alpha_m})}{1 - \exp\left[\frac{B_{\alpha_m} - V_k}{C_{\alpha_m}}\right]} \cdot Q_{10,\alpha_m}^{\frac{T-T0}{10}} \quad (2.20)$$

$$\beta_{m,k} = \frac{A_{\beta_m}(B_{\beta_m} - V_k)}{1 - \exp\left[\frac{V_k - B_{\beta_m}}{C_{\beta_m}}\right]} \cdot Q_{10,\beta_m}^{\frac{T-T0}{10}} \quad (2.21)$$

$$\alpha_{h,k} = \frac{A_{\alpha_h}(B_{\alpha_h} - V_k)}{1 - \exp\left[\frac{V_k - B_{\alpha_h}}{C_{\alpha_h}}\right]} \cdot Q_{10,\alpha_h}^{\frac{T-T0}{10}} \quad (2.22)$$

$$\beta_{k,k} = \frac{A_{\beta_h}}{1 + \exp\left[\frac{B_{\beta_h} - V_k}{C_{\beta_h}}\right]} \cdot Q_{10,\beta_h}^{\frac{T-T0}{10}} \quad (2.23)$$

$$\alpha_{n,k} = \frac{A_{\alpha_n}(V_k - B_{\alpha_n})}{1 - \exp\left[\frac{B_{\alpha_n} - V_k}{C_{\alpha_n}}\right]} \cdot Q_{10,\alpha_n}^{\frac{T-T0}{10}} \quad (2.24)$$

$$\beta_{n,k} = \frac{A_{\beta_n}(B_{\beta_n} - V_k)}{1 - \exp\left[\frac{V_k - B_{\beta_n}}{C_{\beta_n}}\right]} \cdot Q_{10,\beta_n}^{\frac{T-T0}{10}} \quad (2.25)$$

Table 2.3. Values of A, B and C used to calculate the activation of a modelled nerve fibre

	m	m	h	h	n	n
A	0.49	1.04	0.09	3.7	0.02	0.05
B	25.41	21	-27.74	56	35	10
C	6.06	9.41	9.06	12.5	10	10

Table 2.4. Parameters for computation of action potentials

Parameter	Unit	Symbol	Value
Length of nodal membrane	cm	l	0.00001
Axonal diameter	cm	d	0.00003
Resistivity of axoplasm	k -cm		0.07
Leak conductance per unit area	k $^{-1}$/cm^2	g_L	25.78
Nodal potassium permeability	cm/s	P_K	0.000067
Nodal sodium permeability	cm/s	P_{na}	0.00172
Intracellular potassium concentration	mmol/cm^3	$[K^+]_i$	141
Extracellular potassium concentration	mmol/cm^3	$[K^+]_o$	4.2
Intracellular sodium concentration	mmol/cm^3	$[Na^+]_i$	10
Extracellular sodium concentration	mmol/cm^3	$[Na^+]_o$	142
Temperature	K	T	310.15
Faraday's constant	F	C/mol	96485
Gas constant	R	mJ/mol/K	8314.41
Internodal lengths First three internodal segments Soma Four segments after soma Last seven segments	m	L_k	 150,150,150 50 150,200, 250,300 350

The values of the parameters A, B and C were taken from the SE model and are given in Table 2.3. The values of other constants which occur in the GSEF equations are listed in Table 2.4.

3.3 Modelling of nerve fibres with degenerated peripheral processes

A recent study has shown that dendritic counts were consistently lower near the organ of Corti than at a location near the spiral ganglion in mice with sensorineural loss similar to humans (White et al., 2000). To determine the effect of degeneration

of the peripheral processes of nerve fibres, simulations were also performed with a truncated version of the GSEF model. The first four internodal sections were truncated, thus representing a nerve fibre with 12 nodes and 11 internodal segments having its terminal in the modiolus close to node n_5 in Figure 2.4.

4 CONCLUSION

The model of the cochlea presented here is a 3-D spiralling model of the implanted cochlea containing much anatomical detail. Except for the location of the spiral ganglion, the model is based on the anatomy of a human cochlea. Similar spiralling models are either for the guinea pig cochlea (much anatomical detail included) (Frijns, Briaire, & Schoonhoven, 2000) or for a simplified human cochlea (Rattay, Leao, & Felix, 2000). A novel technique is used to incorporate various electrode geometries at two electrode array locations (medial and lateral in the scala tympani relative to the modiolus). Activation of a specific array, electrode geometry and electrode configuration is effected by simply changing the appropriate elements' material properties, i.e. remeshing of model entities is not required. The model can thus be used to investigate electrode configurations and geometries currently used in cochlear implants, as well as experimental electrode configurations and geometries. A layer of scar tissue is also incorporated in the FE model and can be activated or deactivated by changing its elements' material properties. The electrical potential distributions at the target auditory nerve fibres as a result of stimulation current injection is the output from the FE model. The FE model is coupled to an auditory nerve fibre model to facilitate the calculation of neural responses from potential distributions. A truncated version of the nerve fibre model is defined to calculate the response of auditory nerve fibres of which the peripheral processes have degenerated.